PHYSICAL REVIEW E VOLUME 61, NUMBER 5 MAY 2000

Colloidal particles in emulsions

Francisco L. Román,* Matthias Schmidt, and Hartmut Löwen
Institut für Theoretische Physik II, Heinrich-Heine-Universität Düsseldorf, Universitätsstrasse 1, D-40225 Düsseldorf, Germany

(Received 2 December 1999)

We propose a statistical mechanical model for colloidal particles suspended in an emulsion of liquid droplets. The particles are modeled as hard spheres. The interaction between droplets is also hard, but the particles are able to penetrate the droplets. A swelling of droplets is taken into account to ensure material conservation of the droplet liquid. Hence the presence of the colloids generates droplet polydispersity. Using computer simulation and liquid state theory, we find that the relative polydispersity exhibits nonmonotonic behavior as a function of the particle packing fraction and can be traced back to hard sphere bulk density fluctuations.

PACS number(s): 82.70.Kj, 61.20.Gy, 05.20.Jj

I. INTRODUCTION

Soft matter is divided into many subdisciplines dealing with membranes, polymers, colloidal suspensions, or emulsions. These systems have in common that they exhibit structure on a mesoscopic length scale and that they include many degrees of freedom, so one is usually interested in the average, statistical behavior. Nevertheless, the physical phenomena as well as the methods employed to understand them may differ substantially from, say, polymers to colloidal suspensions. Insight can be gained by investigating systems that bridge such areas. In the present work we investigate the interplay between colloidal suspensions and liquid emulsions.

Suspensions of colloidal particles are mixtures between a molecular solvent and mesoscopic solid particles [1]. The latter are often loosely called ''colloids.'' Apart from effects of gravity like sedimentation, the colloids float in their solvent liquid and interact with each other in similar ways to the interaction of atoms in ''hard'' condensed matter. The important and interesting difference is the large variety of interaction potentials present between colloidal particles. These interactions are effective in the sense that they arise from underlying microscopic mechanisms like van der Waals forces, Coulomb forces, or the Born repulsion. One simple theoretical model for the treatment of these systems is the hard sphere model, namely, a collection of spherical particles that cannot interpenetrate each other. It is the generic model to understand dense fluids and crystalline solids. Surprisingly, it is realized in nature in suspensions of sterically stabilized colloidal particles. By matching the refractive indices of the solvent with the colloid material, it is possible to turn down the van der Waals attraction. The particles are coated with short polymer brushes needed to stabilize the suspension against coagulation of particles. As the polymer brushes are tiny compared to the particle diameter, which is of the order of microns, a repulsive potential emerges that is almost hard-sphere-like. There is also considerable current activity in the field of computer simulations of colloids [2].

Hard spheres are also considered as a model for the second area we want to cover, namely, liquid emulsions. These are mixtures of two (or more) liquid phases, one being the continuous phase that contains droplets of the dispersed phase(s). The droplets can be very well controlled to have unique sizes [3] so that even freezing occurs. Although both dispersed particles and dispersed droplets float in a surrounding liquid, the important difference is that the dispersed objects in emulsions are in the fluid rather than in the solid state.

In the present work, we investigate a mixture of colloidal particles and emulsion droplets; see Fig. 1 for a schematic sketch of the physical situation. Therefore we propose and study a model system. This system is simplified in many respects, but it keeps the freedom for the particles to choose between being dissolved in the continuous phase or within a dispersed droplet. In reality, the surface tensions between the colloid material and both solvents will determine whether the colloids tend to aggregate within or become depleted from the droplets. There is, however, an even more fundamental mechanism based on material conservation that we aim at. As we consider the emulsion on a small time scale, where no coalescence of droplets appears, we are faced with the fact that the amount of the dispersed phase (oil) and that of the continuous phase (water) are conserved quantities. These constraints lead to a nontrivial behavior of the droplet sizes. As particles penetrate inside an empty droplet, the droplet size (diameter) has to grow, in order to keep the oil volume constant. The present work aims at the study of the emerging droplet size distribution, its polydispersity, and the structural correlations present in the system.

There are important phenomena present in emulsions that are neglected within the current approach. Here, we deal only with perfect spherical droplets. Fluctuations of the drop-

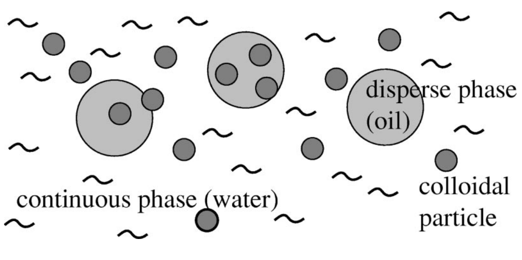

FIG. 1. Physical system of colloidal particles suspended in an emulsion. The different components are colloids (small spheres), emulsion droplets (big spheres), and solvent (wiggles). Particles can penetrate inside droplets.

---

*Present address: Departamento de Física Aplicada, Facultad de Ciencias, Universidad de Salamanca, E-37008 Salamanca, Spain.

1063-651X/2000/61(5)/5445(7)/$15.00

let shape [4,5] are ignored. Denkov *et al.* [6] have considered colloidal particles pinned at the surface of emulsion droplets and have proposed that this coating may lead to stabilization of the emulsion against coalescence. Similar to our current study is the theoretical work on colloids suspended in a two-phase solvent [7,8] and measurements of the phase behavior of colloids in binary liquid mixtures [9]. In our system, however, both liquids are in a metastable emulsion state. This enables the preparation of spherical droplets of one phase within the other, which is not the case in the above mentioned bulk systems.

The study of polydisperse systems, especially polydisperse hard spheres, has attracted a lot of recent interest; see, e.g., [10–13]. In these studies, the distribution of sphere sizes is an input quantity, and the impacts on phenomena like freezing are investigated. In the present work, however, the polydispersity is generated through material conservation and hence is an output quantity.

Our system has two components with hard sphere interactions among like species. However, as our results will show, it is quite dissimilar from a binary additive hard sphere mixture, which has also attracted a lot of recent interest (see, e.g., [14]). We note that this system has been prepared experimentally using either colloids (see, e.g., [15]) or binary emulsions (see, e.g., [16]). Hence, it is conceivable that experimentalists will be able to prepare well-defined mixtures of droplets and colloids, which are the issue of interest of the present work.

In Sec. II the model for colloidal particles suspended in an emulsion is proposed. Then a theoretical approach linking density fluctuations to polydispersity is presented in Sec. III. Various limiting cases are discussed. Section IV explains the Monte Carlo simulation method, and results are given in Sec. V. We finish with concluding remarks in Sec. VI.

II. THE MODEL

We consider a mixture of two components. One component is made of N_C monodisperse hard spheres, called colloids, with diameters σ_C and position vectors $\mathbf{r}_{C,i}$, where $i=1,\ldots,N_C$. They interact with a pairwise hard core potential

$$\phi_{CC}(r_{C,ij})=\begin{cases}\infty & \text{if } r_{C,ij}<\sigma_C\\ 0 & \text{otherwise,}\end{cases}\tag{1}$$

where $r_{C,ij}=|\mathbf{r}_{C,i}-\mathbf{r}_{C,j}|$ is the separation distance between colloids i and j.

The second component is constituted of N_D droplets with polydisperse diameters $\sigma_{D,k}$, $k=1,\ldots,N_D$, and position vectors $\mathbf{r}_{D,k}$. Again, the interaction between droplets is pairwise hard core,

$$\phi_{DD}(r_{D,kl})=\begin{cases}\infty & \text{if } r_{D,kl}<\frac{1}{2}(\sigma_{D,k}+\sigma_{D,l})\\ 0 & \text{otherwise,}\end{cases}\tag{2}$$

where $r_{D,kl}=|\mathbf{r}_{D,k}-\mathbf{r}_{D,l}|$ is the separation distance between droplets k and l. The total system volume is V_0.

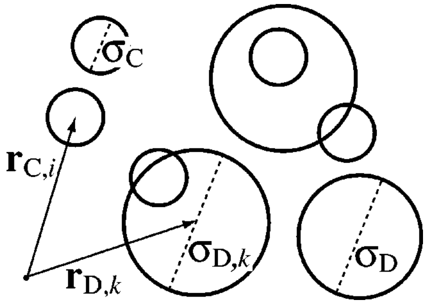

FIG. 2. Theoretical model of colloids in emulsions containing colloids (small circles) with positions $\mathbf{r}_{C,i}$ and diameters σ_C, and droplets (large circles) with positions $\mathbf{r}_{D,k}$. The diameter of an empty droplet is σ_D; the actual diameter of the kth droplet is denoted by $\sigma_{D,k}$.

For each set of particle positions $\{\mathbf{r}_{C,i}\}$, the droplet radius of the kth droplet at position $\mathbf{r}_{D,k}$ is determined by material conservation, expressed as

$$\frac{\pi}{6}\sigma_{D,k}^3=\frac{\pi}{6}\sigma_D^3+\int d^3x\,\Theta\left(\frac{\sigma_{D,k}}{2}-|\mathbf{x}-\mathbf{r}_{D,k}|\right)\times\sum_{i=1}^{N_D}\Theta\left(\frac{\sigma_C}{2}-|\mathbf{x}-\mathbf{r}_{C,i}|\right),\tag{3}$$

where $\Theta(x)$ is the Heaviside step function. The diameter of an empty droplet is σ_D. Equation (3) expresses the fact that the volume of a swollen droplet equals the volume of an empty droplet plus the volume of particles inside the droplet. The latter is expressed as an integration over a function that is unity for space points $\mathbf{x}$ that are both inside a particle and inside a droplet, and vanishes otherwise. The total potential energy is

$$\phi_{\text{total}}=\sum_{i<j=1}^{N_C}\phi_{CC}(r_{C,ij})+\sum_{k<l=1}^{N_D}\phi_{DD}(r_{D,kl}).\tag{4}$$

In Fig. 2 the model is sketched.

Next we introduce dimensionless quantities that govern the system. The packing fractions of colloids and of droplets are defined as

$$\eta_C=\frac{N_C\pi}{6V_0}\sigma_C^3,\tag{5}$$

$$\eta_D=\frac{N_D\pi}{6V_0}\sigma_D^3.\tag{6}$$

The third reduced parameter is the size ratio σ_D/σ_C of the diameter of colloids and empty droplets.

III. THEORY

As the droplet size distribution is not prescribed *a priori* in our model, we have to find means to analyze it. Therefore we will develop a theory for the calculation of the polydispersity of the emulsion. The droplet size distribution is defined by

$$p(\sigma)=\left\langle \frac{1}{N_D}\sum_{k=1}^{N_D} \delta(\sigma-\sigma_{D,k})\right\rangle, \tag{7}$$

where $\langle\cdots\rangle$ denotes a canonical average with the total potential energy given in Eq. (4).

The polydispersity s is the standard deviation of the droplet size distribution divided by the mean (see, e.g., [17,18]),

$$s=\frac{\sqrt{(m_2-m_1^2)}}{m_1}, \tag{8}$$

where m_i are moments of the droplet size distribution $p(\sigma)$,

$$m_i=\int_0^\infty d\sigma p(\sigma)\sigma^i. \tag{9}$$

The calculation of the polydispersity requires knowledge of the moments m_1 and m_2 of the distribution $p(\sigma)$. Since in our system the droplet diameter σ is related (via material conservation) to the number N of colloids inside the droplet, we shall use this relation to obtain approximate expressions for m_1 and m_2. Explicitly, material conservation implies

$$N=\frac{\sigma^3-\sigma_D^3}{\sigma_C^3} \tag{10}$$

and then

$$\langle N\rangle=\frac{m_3-\sigma_D^3}{\sigma_C^3} \tag{11}$$

and

$$\langle N^2\rangle-\langle N\rangle^2=\frac{m_6-m_3^2}{\sigma_C^6}, \tag{12}$$

where we have used the identity $m_k=\langle\sigma^k\rangle$. Expressions (11) and (12) are exact but difficult to handle since they involve the moments m_3 and m_6. These moments can be related to m_1 and m_2 if we assume that $p(\sigma)$ can be approximated by a Gaussian of mean m_1 and standard deviation $\sqrt{m_2-m_1^2}=m_1 s$. We obtain

$$\langle N\rangle=\frac{1}{\sigma_C^3}(m_1^3+3s^2m_1^3-\sigma_D^3), \tag{13}$$

$$\langle N^2\rangle-\langle N\rangle^2=\frac{1}{\sigma_C^6}3s^2m_1^6(3+12s^2+5s^4), \tag{14}$$

which are our final expressions for linking the polydispersity s and the first moment m_1 to the average number of particles in a droplet and its fluctuations. In the following subsection we consider the case of low emulsion density where one can address suitable approximations for the relative fluctuation $(\langle N^2\rangle-\langle N\rangle^2)/\langle N\rangle$ and the moment m_1 that will allow us to obtain the polydispersity of the droplets.

A. The limit of low droplet densities

For low droplet densities $\eta_D\rightarrow 0$, the interaction between emulsion droplets can be neglected. The interaction in our system is such that the colloidal particles are undisturbed by the presence of the droplet. Then the colloids form a simple bulk hard sphere system, which is, of course, monodisperse. We can therefore obtain the moment m_1 (the mean diameter of the droplets) from the following material conservation expression [see Eq. (3)]:

$$\frac{\pi}{6}m_1^3(1-\eta_C)=\frac{\pi}{6}\sigma_D^3. \tag{15}$$

Moreover, if we consider a droplet with volume $V=\pi\sigma^3/6$ then it is possible to write the fluctuation in the number of colloidal particles inside the droplet as

$$\frac{\langle N^2\rangle-\langle N\rangle^2}{\langle N\rangle}=1+\frac{\rho_C}{V}\int_V\int_V d\mathbf{r}d\mathbf{r}'[g_{CC}(|\mathbf{r}-\mathbf{r}'|)-1], \tag{16}$$

where $\rho_C=6\eta_C/\pi\sigma_C^3$ is the number density of the colloid and g_{CC} is the uniform fluid pair distribution function of the colloid. When the size V of the droplets becomes very large, Eq. (16) can be written in terms of the isothermal compressibility of the colloid χ_T,

$$\lim_{V\rightarrow\infty}\frac{\langle N^2\rangle-\langle N\rangle^2}{\langle N\rangle}=\rho_C k_B T\chi_T, \tag{17}$$

where k_B is Boltzmann's constant and T is the temperature of the system. However, for small droplets finite size effects arise (see, e.g., Refs. [19], [20]) and one must take into account the limits of integration in Eq. (16).

The procedure for the calculation of Eq. (16) follows the same basic ideas of Refs. [21], [19], [20]. First we write Eq. (16) in Fourier space,

$$\frac{\langle N^2\rangle-\langle N\rangle^2}{\langle N\rangle}=1+\frac{\rho_C}{(2\pi)^3V}\int d\mathbf{k}\hat{G}^2(\mathbf{k})\hat{h}(\mathbf{k}), \tag{18}$$

where $\hat{G}(\mathbf{k})$ is the Fourier transform of a geometry function that accounts for the limits of integration (it is 1 inside the droplet and zero otherwise), and $\hat{h}(\mathbf{k})$ is the Fourier transform of the total correlation function $h(\mathbf{r})=g(\mathbf{r})-1$. Then, taking into account that $G(\mathbf{r})$ is a sphere of diameter σ, we get

$$\hat{G}(\mathbf{k})=\hat{G}(k)=\frac{4\pi}{k^3}\left[\sin\left(\frac{k\sigma}{2}\right)-\frac{k\sigma}{2}\cos\left(\frac{k\sigma}{2}\right)\right]. \tag{19}$$

On the other hand, we use the Ornstein-Zernike relation for the total correlation function

$$\hat{h}(k)=\frac{\hat{c}(k)}{1-\rho_C\hat{c}(k)}, \tag{20}$$

where $\hat{c}(k)$ is the Fourier transform of the direct correlation function. For simplicity, we use the Percus-Yevick solution for the direct correlation function since in this case we obtain analytical results for $\hat{h}(k)$ and the fluctuations (18). In our system the diameter σ is not a constant but depends on the number of particles inside the droplet. As an approximation we consider the following effective diameter:

$$\overline{\sigma} = m_1 + \sigma_C, \tag{21}$$

where σ_C accounts for the size of the colloids. From Eq. (21) we obtain

$$V = \frac{\pi}{6}(m_1 + \sigma_C)^3. \tag{22}$$

In summary, the calculation of the polydispersity for the low density case is as follows. First we use Eq. (15) to obtain m_1. Then, from Eqs. (22) and (18) we calculate the fluctuations $(\langle N^2\rangle - \langle N\rangle^2)/\langle N\rangle$. Finally, making use of Eqs. (13) and (14) we solve

$$\frac{\langle N^2\rangle - \langle N\rangle^2}{\langle N\rangle} = \frac{1}{\sigma_C^3}\,\frac{3s^2 m_1^6(3+12s^2+5s^4)}{m_1^3 + 3s^2 m_1^3 - \sigma_D^3} \tag{23}$$

to obtain the polydispersity s.

B. Intermediate and high emulsion densities

For high or intermediate densities of the emulsion, the interaction between droplets cannot be neglected. This interaction has an impact on the colloidal fluid. Thus the effective volume of the droplet used in expression (18) cannot be calculated as in Eq. (15), since in this case it depends not only on the mean density of colloidal particles but also on the density of the emulsion droplets. Because of this inhomogeneous character of the density of the colloid, we have not derived theoretical results for the polydispersity.

However, on the basis of the behavior at low density, it is possible to argue about the behavior of the polydispersity at higher emulsion densities. On the one hand, the exclusion interaction between droplets does not allow for the possibility of growth, but, on the other hand, at intermediate and high densities the colloid particles do not allow for the shrinking of the droplets. As a consequence, we expect that the probability distribution $p(\sigma)$ should become narrow and then the polydispersity should decrease. As we shall see below, this will be confirmed from results of computer simulation. These simulation results indicate that, for a given fixed colloid density, the low emulsion density result provides an upper bound for the polydispersity of the emulsion.

IV. COMPUTER SIMULATION

A. Monte Carlo technique

From a general viewpoint, the simulation handles two coupled systems. One is the emulsion droplet system, which is a polydisperse system of hard spheres of variable diameters $\{\sigma_{D,i}\}_{i=1,\ldots,N_D}$. The other is the colloid system, which consists of a standard monodisperse hard sphere system with particles of diameter σ_C. Both, the emulsion droplets and colloidal particles are coupled via the interaction potential (4).

The simulation runs with a fixed number of emulsion droplets N_D and a fixed number of colloidal particles N_C. In accordance with the standard Monte Carlo method, one proceeds as follows. First, one particle is randomly chosen (it can be either a droplet or a colloid particle) and a random displacement is proposed. The test for acceptance or rejection of the move depends on the energy change. As we are dealing with a hard potential, the energy change is either zero (if no overlapping situation is reached) or infinity (when there is an overlap). In the former case the state is accepted, in the latter it is rejected. The overlapping states can be reached because of both the simple movement of a particle or the growth of a droplet due to the inclusion of colloidal particles.

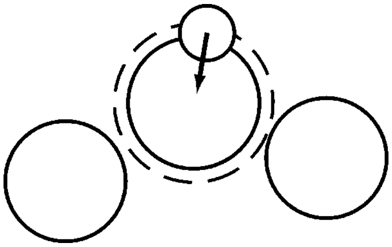

FIG. 3. Swelling of droplets. If a colloidal particle tries to move (arrow) inside a droplet, the swelling of the droplet happens against the pressure of the surrounding droplets.

After proposing a new position for a droplet or colloid, it is necessary to calculate the new diameters for the droplets in order to test for possible overlapping situations. This is done by means of conservation of both the total amount of material in the droplets and the positions of the centers of the droplets. The growth for the droplets is isotropic with respect to the center of each droplet (see Fig. 3).

The algorithm for calculating the new proposed diameter of the droplet is as follows. Let us suppose that a trial move is proposed for the droplet j with diameter $\sigma_{D,j}$ and position $r_{D,j}$, and the proposed position for this droplet is $\mathbf{r}_{D,j}^*$. In order to calculate its new diameter $\sigma_{D,j}^*$, we solve the equation

$$\frac{\pi}{6}(\sigma_{D,j}^*)^3 - \sum_{i=1}^{N_C} I(|\mathbf{r}_{D,j}^* - \mathbf{r}_{C,i}|, \sigma_C, \sigma_{D,j}^*) - \frac{\pi}{6}\sigma_D^3 = 0, \tag{24}$$

where I is the intersection volume between particle i and the displaced droplet j. The geometrical function I is given for two intersecting spheres with center separation distance r and diameters $\sigma_1, \sigma_2 (\sigma_1 < \sigma_2)$ by

$$I(r,\sigma_1,\sigma_2) = \begin{cases} \pi\sigma_1^3/6 & \text{if } r \leqslant (\sigma_2 - \sigma_1)/2 \\ L(r,\sigma_1,\sigma_2) & \text{if } (\sigma_2-\sigma_1)/2 < r \leqslant (\sigma_2+\sigma_C)/2 \\ 0 & \text{otherwise,} \end{cases} \tag{25}$$

where the auxiliary function L is the volume of a lenslike shape and is given by

$$L(r,\sigma_1,\sigma_2) = \frac{\pi}{12r}\left(\frac{\sigma_2+\sigma_1}{2} - r\right)^2 \times\left[r^2 - 3\left(\frac{\sigma_2-\sigma_1}{2}\right)^2 + 2r\left(\frac{\sigma_2+\sigma_1}{2}\right)\right]. \tag{26}$$

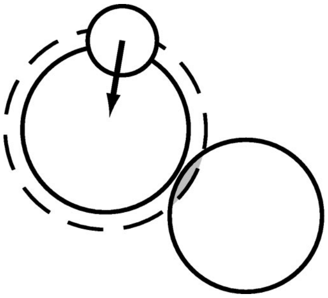

FIG. 4. Overlap due to swelling. A colloidal Monte Carlo move (indicated by an arrow) may be rejected, because the swollen droplet would overlap (shaded region) with another droplet.

In practice, the terms that actually contribute to the sum over i in Eq. (24) are selected through a neighbor list.

Once the new diameter is calculated, the next step is to verify whether an overlapping situation is reached. Fig. 4 shows that it is possible to reject a colloid particle displacement because of droplet growth. This is also possible if a droplet is displaced in such a way that its growth leads to an overlap with a neighboring droplet. Then the displacement has to be rejected. Of course, situations in which a colloidal particle can interact with two or even more droplets are possible, and it is necessary to calculate the final diameter of each droplet before testing for droplet overlaps.

B. Simulation details

Several simulations for different values of the parameters η_C and η_D have been performed to obtain the behavior of the polydispersity of the emulsion droplets. In all of the simulations the size ratio is $\sigma_D/\sigma_C=3$. A typical run starts from a face-centered cubic lattice of $N_D=32$ droplets and a given number of colloidal particles N_C ranging from 50 to 1000. The number of Monte Carlo steps (MCS) used to thermalize the system is 10^7. After that the probability distribution function $p(\sigma)$ as well as the pair correlation functions are measured during 10^8 MCS. Finally, the polydispersity is calculated by using Eq. (8).

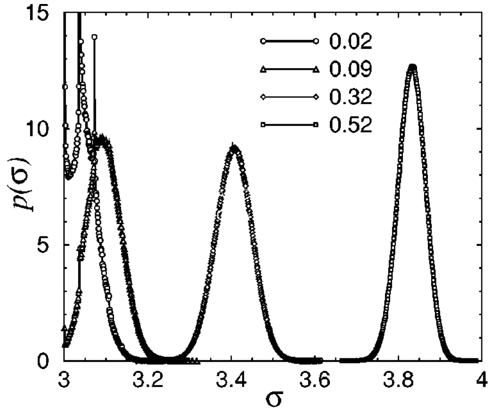

FIG. 5. The diameter probability distribution $p(\sigma)$ for a system with a single emulsion droplet and various packing fractions of the colloid $\eta_C=0.02$, 0.09, 0.32, 0.52, and size ratio $\sigma_D/\sigma_C=3$. As the packing fraction of colloid increases, the width of the distribution (polydispersity) decreases.

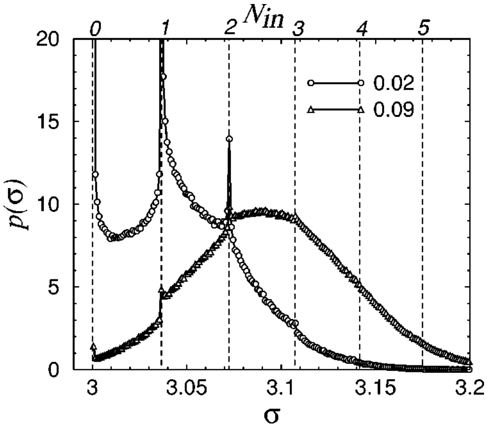

FIG. 6. Detail of Fig. 5. Note the probability spikes corresponding to integer numbers $N_{\rm in}$ of colloid particles inside the droplet.

V. RESULTS

A. Intrinsic polydispersity

The behavior of the probability distribution function $p(\sigma)$ for several colloid densities $\eta_C=0.02, 0.09, 0.32, 0.52$ is shown in Fig. 5. We consider the case of infinite dilution of droplets, namely, a system with a single droplet. For large colloid packing fractions, nearly Gaussian behavior for $p(\sigma)$ emerges. The mean value grows upon increasing η_C, reflecting the size of a typically swollen droplet. The width of the distribution, however, decreases upon increasing the colloid density from $\eta_C=0.32$ to 0.52. The underlying mechanism is the reduction of bulk hard sphere density fluctuations for the dense colloidal fluid.

The Gaussian picture, however, breaks down for low densities of colloids, $\eta_C=0.02$ and 0.09 (see Fig. 6). A hump-like shape is still present, but there arise additional spikes. We find that these spikes appear in the distribution when an integer number of particles $N_{\rm in}$ is completely inside the droplet so that no particle intersects with the droplet surface. This happens at $\sigma/\sigma_C=[(\sigma_D/\sigma_C)^3+N_{\rm in}]^{1/3}$, where $N_{\rm in}$ is an integer or zero. As an explanation for this droplet size distribution, we note that the number of states with one particle

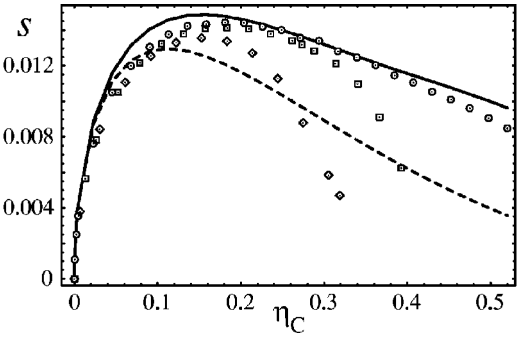

FIG. 7. Polydispersity s of the droplets versus the packing fraction of the colloid η_C. Circles, squares, and diamonds represent the simulation data obtained for systems of one droplet, $\eta_D=0.45$, and $\eta_D=0.53$, respectively. The solid line represents the theoretical results coming from Eq. (18). The dashed line represents Eq. (17) (when the size of the droplet is very large). Note that the very low density case (one droplet) is an upper bound for the polydispersity. The size ratio is $\sigma_D/\sigma_C=3$.

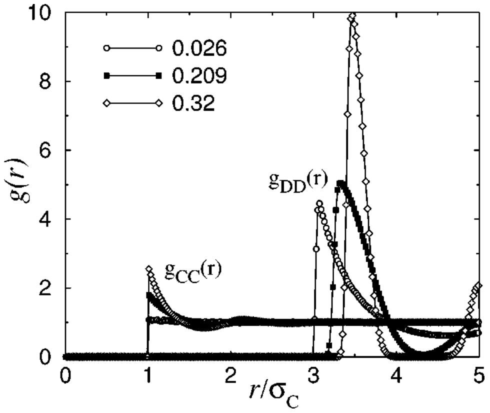

FIG. 8. Distribution functions of colloidal pairs $g_{CC}(r)$ and droplet pairs $g_{DD}(r)$. The droplet packing fraction is $\eta_D = 0.452$. Three concentrations for colloids are shown, $\eta_C = 0.026$, 0.209, 0.314. Lines are guides to the eye.

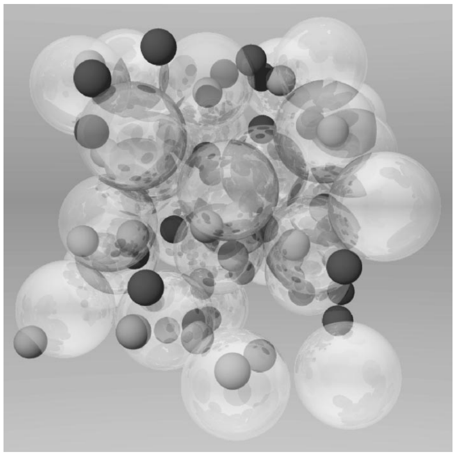

FIG. 10. Snapshot from computer simulation. The large transparent spheres are droplets, the smaller ones represent colloidal particles. A colloid is shaded dark if its center is not inside any droplet. The packing fractions are $\eta_C = 0.026$, $\eta_D = 0.452$. The droplet subsystem is in a fluid state.

inside the droplet (proportional to the volume of one sphere of diameter $\sigma_D - \sigma_C/2$) will be greater than the number of states with one particle intersecting the surface of the droplet (proportional to the surface of the droplet). For higher densities of colloid, the presence of more particles located at the border of the droplet smooths the behavior of the probability distribution. This leads to a highly nontrivial size distribution that consists of finite probabilities at discrete diameter values with a superimposed continuous probability density that interpolates between the spikes.

In order to condense the information, we study the width of the distribution as a function of the thermodynamic parameters. Figure 7 shows the simulation results for the polydispersity versus the packing fraction of the colloid. Circles correspond to the case of one emulsion droplet in the system, squares and diamonds correspond, respectively, to packing fractions of the emulsion droplets $\eta_D = 0.45$ and $\eta_D = 0.53$. We observe that the case of low emulsion densities is an upper bound for the polydispersity. Its behavior is as follows. All points start from the value zero that corresponds to a monodisperse emulsion. As the density increases, more colloidal particles are added to the system and, as a consequence of that, the polydispersity increases up to a maximum value. When still more colloid particles are added, the polydispersity decreases since the colloid system approaches a dense liquid or even solid phase, and fluctuations in the number of particles inside a droplet decrease. We have found that, as the density of the emulsion increases, it is not possible to reach high colloid densities. This is due to the exclusion interaction for the droplets since the more colloid is added, the bigger the emulsion droplets become, and it is even possible to freeze the emulsion.

Solid and dashed lines in Fig. 7 represent the theoretical results obtained from Eqs. (18) and (17), respectively. Note that our incorporation of finite size effects improves on the result for the thermodynamic limit. We get good agreement for the case of low emulsion density. Differences between simulation results and results obtained by using Eqs. (18) and (23) have a different origin depending on the colloid density. For low colloid densities, our Gaussian approximation for $p(\sigma)$ breaks down (see Fig. 6.) For the high colloid density case, deviations arise partly because of the Percus-Yevick form of the total correlation function in Eq. (18) and

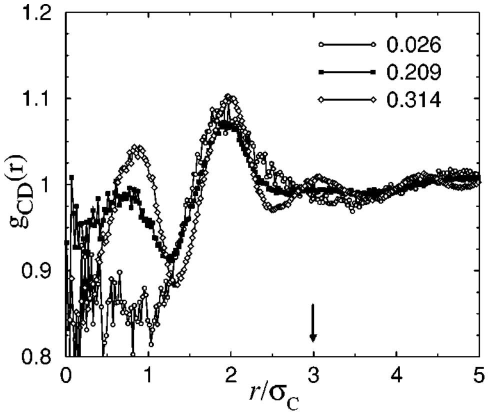

FIG. 9. Distribution function for colloid-droplet pairs $g_{CD}(r)$, for the same parameters as in Fig. 8. The arrow denotes the radius of an empty droplet. Note the different ordinate scale compared to Fig. 8.

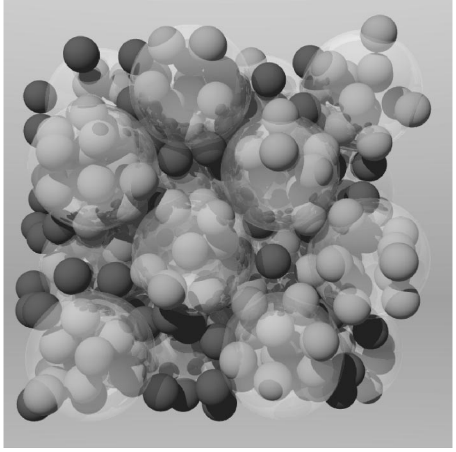

FIG. 11. Same as Fig. 10, but at a higher particle volume fraction $\eta_C = 0.314$. The droplets are frozen on a face-centered cubic lattice, while the colloids remain liquid.

mainly because the volume V in Eq. (18) is approximated by that of a sphere of the mean diameter of the droplets.

B. Structural correlations

As the system has two components, one can investigate three different static pair distributions. First, we discuss the symmetric correlations $g_{CC}(r)$ between colloidal pairs and $g_{DD}(r)$ between droplet pairs (see Fig. 8). The packing fraction of the droplets is high, $\eta_D = 0.452$, and there are three cases of particle packing fractions shown, namely, $\eta_C = 0.026, 0.209, 0.314$. The behavior of the colloids is similar to that of monodisperse hard spheres, except for a slight shift of the second peak toward larger distances compared to the one-component system. The droplet behavior is also hard-sphere-like but the intrinsic polydispersity washes out the first peak. At the largest values of $\eta_C = 0.314$, the droplet subsystem is found to be in a crystalline state.

A quite different behavior is found for the asymmetric correlations between pairs of one particle and one droplet, $g_{CD}(r)$, Fig. 9. This distribution function can be regarded as the density profile of particles inside (and around) a fixed droplet. Of course, it also has the meaning of the density profile of droplets around a fixed particle. There are weak oscillations inside one droplet radius, which become rapidly damped outside. The amplitude of the oscillations is tiny, even at the highest packing fraction considered. The behavior is dissimilar from that of a hard sphere fluid inside a hard cavity [22–25], where much stronger structure emerges.

To illustrate our findings we show snapshots generated from the simulation. In Fig. 10 the high density droplet liquid phase containing few particles is shown. By adding more particles, freezing of the droplet system occurs, Fig. 11. The bare droplet packing fraction of $\eta_D = 0.452$ is well inside the fluid branch of the hard sphere phase diagram. The swollen droplets, however, build a nearly close-packed face-centered cubic crystal.

VI. CONCLUSIONS

A model for the behavior of emulsions in the presence of colloidal particles has been proposed. It describes colloids as monodisperse hard spheres and emulsion droplets as polydisperse hard spheres. Migration of colloids into and out of the droplets is allowed. The droplet size distribution is not assumed *a priori*, but evolves self-consistently. Therefore interactions between colloidal particles and emulsion droplets are taken into account so that conservation of the emulsion droplet material is fulfilled. Then the exclusion rule of hard spheres drives the droplet size distribution. We show that this distribution has quite a rich structure, ranging from multispike to Gaussian behavior. By means of the study of the size dependent fluctuations in the number of particles located inside the droplets, we found an upper bound for the polydispersity of the emulsion.

Concerning future work, we remark that the present model may be readily generalized to account for nonvanishing surface tensions. In general, there are three surface tensions between the three materials, colloid, oil, and water. Within the current approach, the surfaces themselves are given geometrically by intersections of spheres. Hence one can take into account the potential energy that comes from the presence of these interfaces. By tuning the surface tensions, one then has additional control over the colloidal tendency to aggregate inside droplets.

ACKNOWLEDGMENTS

We thank Lutz Maibaum, Holger M. Harreis, and Juan A. White for valuable contributions. F.L.R. acknowledges the financial support from the Dirección General de Investigación Científica y Técnica (DGICYT) of Spain under Grant Nos. PB 95-0934 and PB 98-0261 and from the Ministerio de Educación y Cultura.

---

[1] H. Löwen, Phys. Rep. **237**, 249 (1994).
[2] M. Schmidt, in *Computational Methods in Colloid and Interface Science*, edited by M. Borówko (M. Dekker, New York, 1999), Chap. 15, p. 745.
[3] T. G. Mason and J. Bibette, Phys. Rev. Lett. **77**, 3481 (1996).
[4] Hu Gang, A. H. Krall, and D. A. Weitz, Phys. Rev. Lett. **73**, 3435 (1994).
[5] W. Cai, Phys. Rev. E **54**, 2780 (1996).
[6] N. D. Denkov, I. B. Ivanov, P. A. Kralchevsky, and D. T. Wasan, J. Colloid Interface Sci. **150**, 589 (1992).
[7] H. Löwen, Phys. Rev. Lett. **74**, 1028 (1995).
[8] H. Löwen, Z. Phys. B: Condens. Matter **97**, 269 (1995).
[9] Y. Jayalakshmi and E. W. Kaler, Phys. Rev. Lett. **78**, 1379 (1997).
[10] P. Bartlett, Mol. Phys. **97**, 685 (1999).
[11] D. A. Kofke and P. G. Bolhuis, Phys. Rev. E **59**, 618 (1999).
[12] R. P. Sear, Phys. Rev. Lett. **82**, 4244 (1999).
[13] J. F. Zhang, R. Blaak, E. Trizac, J. A. Cuesta, and D. Frenkel, J. Chem. Phys. **110**, 5318 (1999).
[14] M. Dijkstra, R. van Roij, and R. Evans, Phys. Rev. Lett. **81**, 2268 (1998).
[15] A. Imhof and J. K. G. Dhont, Phys. Rev. Lett. **75**, 1662 (1995).
[16] U. Steiner, A. Meller, and J. Stavans, Phys. Rev. Lett. **74**, 4750 (1995).
[17] H. Löwen, J.-N. Roux, and J.-P. Hansen, J. Phys.: Condens. Matter **3**, 997 (1991).
[18] P. N. Pusey, J. Phys. (France) **48**, 709 (1987).
[19] F. L. Román, J. A. White, and S. Velasco, J. Chem. Phys. **107**, 4635 (1997).
[20] F. L. Román, A. González, J. A. White, and S. Velasco, J. Chem. Phys. **110**, 9821 (1999).
[21] J. J. Salacuse, A. R. Denton, and P. A. Egelstaff, Phys. Rev. E **53**, 2382 (1996).
[22] A. González, J. A. White, F. L. Román, S. Velasco, and R. Evans, Phys. Rev. Lett. **79**, 2466 (1997).
[23] A. González, J. A. White, F. L. Román, and R. Evans, J. Chem. Phys. **109**, 3637 (1998).
[24] Z. T. Németh and H. Löwen, J. Phys.: Condens. Matter **10**, 6189 (1998).
[25] Z. T. Németh and H. Löwen, Phys. Rev. E **59**, 6824 (1999).